A coupled model of the global cycles of carbonyl sulfide and CO_2: A possible new window on the carbon cycle

Joe Berry,[1] Adam Wolf,[2] J. Elliott Campbell,[3] Ian Baker,[4] Nicola Blake,[5] Don Blake,[5] A. Scott Denning,[4] S. Randy Kawa,[6] Stephen A. Montzka,[7] Ulrike Seibt,[8] Keren Stimler,[9] Dan Yakir,[9] and Zhengxin Zhu[6]

Received 3 July 2012; revised 26 April 2013; accepted 2 May 2013.

[1] Carbonyl sulfide (COS) is an atmospheric trace gas that participates in some key reactions of the carbon cycle and thus holds great promise for studies of carbon cycle processes. Global monitoring networks and atmospheric sampling programs provide concurrent data on COS and CO_2 concentrations in the free troposphere and atmospheric boundary layer over vegetated areas. Here we present a modeling framework for interpreting these data and illustrate what COS measurements might tell us about carbon cycle processes. We implemented mechanistic and empirical descriptions of leaf and soil COS uptake into a global carbon cycle model (SiB 3) to obtain new estimates of the COS land flux. We then introduced these revised boundary conditions to an atmospheric transport model (Parameterized Chemical Transport Model) to simulate the variations in the concentration of COS and CO_2 in the global atmosphere. To balance the threefold increase in the global vegetation sink relative to the previous baseline estimate, we propose a new ocean COS source. Using a simple inversion approach, we optimized the latitudinal distribution of this ocean source and found that it is concentrated in the tropics. The new model is capable of reproducing the seasonal variation in atmospheric concentration at most background atmospheric sites. The model also reproduces the observed large vertical gradients in COS between the boundary layer and free troposphere. Using a simulation experiment, we demonstrate that comparing drawdown of CO_2 with COS could provide additional constraints on differential responses of photosynthesis and respiration to environmental forcing. The separation of these two distinct processes is essential to understand the carbon cycle components for improved prediction of future responses of the terrestrial biosphere to changing environmental conditions.

Citation: Berry, J., et al. (2013), A coupled model of the global cycles of carbonyl sulfide and CO_2: A possible new window on the carbon cycle, *J. Geophys. Res. Biogeosci.*, *118*, doi:10.1002/jgrg.20068.

1. Introduction

[2] Carbonyl sulfide (COS) is an atmospheric trace gas that holds great promise for studies of carbon cycle processes [*Blonquist et al.*, 2011; *Campbell et al.*, 2008; *Montzka et al.*, 2007; *Seibt et al.*, 2010; *Suntharalingam et al.*, 2008; *Wohlfahrt et al.*, 2012]. COS is an analog of carbon dioxide (CO_2). It participates in some key reactions of the carbon cycle, and its concentration, like that of the ^{13}C and ^{18}O isotopologues of CO_2, provides additional information on carbon cycle processes. Specifically, COS is taken up by reactions associated with leaf photosynthesis and microbial activity in soils. Unlike for CO_2, soils are generally a sink for COS [*Van Diest and Kesselmeier*, 2008]. The drawdown of COS concentration over the continents is, therefore, related to the sum of photosynthesis and soil microbial activity, while that of CO_2 is related to the difference between net photosynthesis and respiration terms. The main source of COS is biogenic activity in the ocean [*Cutter et al.*, 2004], and uptake by leaves and soil are its main sink.

[1]Department of Global Ecology, Carnegie Institution, Stanford, California, USA.
[2]Department of Ecology and Evolutionary Biology, Princeton University, Princeton, New Jersey, USA.
[3]Sierra Nevada Research Institute, University of California, Merced, Merced, California, USA.
[4]Department of Atmospheric Science, Colorado State University, Fort Collins, Colorado, USA.
[5]Department of Chemistry, University of California, Irvine, Irvine, California, USA.
[6]NASA Goddard Space Flight Center, Greenbelt, Maryland, USA.
[7]NOAA Earth System Research Laboratory, Boulder, Colorado, USA.
[8]Department of Atmospheric and Oceanic Sciences, University of California, Los Angeles, Los Angeles, California, USA.
[9]Environmental Sciences and Energy Research, Weizmann Institute of Science, Rehovot, Israel.

Corresponding author: J. Berry, Department of Global Ecology, Carnegie Institution, Stanford, CA 94305, USA. (joeberry@stanford.edu)

2169-8953/13/10.1002/jgrg.20068

Table 1. A Compilation of the Global Sources and Sinks Used for PCTM Simulations of Atmospheric COS[a]

Sources	*Kettle et al.*, 2002	This Study
Direct COS Flux From Oceans	39	39
Indirect COS Flux as DMS From Oceans	81	81
Indirect COS Flux as CS_2 From Oceans	156	156
Direct Anthropogenic Flux	64	64
Indirect Anthropogenic Flux From CS_2	116	116
Indirect Anthropogenic Flux From DMS	0.5	0.5
Biomass Burning	11	**136**
Additional (Photochemical) Ocean Flux		**600**
Sinks		
Destruction by OH Radical	−94	**−101**
Uptake by Canopy	−238	**−738**
Uptake by Soil	−130	**−355**
Net Total	−5	−2.5

[a]Units are 1.0×10^9 g of sulfur. Fluxes changed in this study are highlighted with bold type.

Atmospheric chemistry and anthropogenic sources, while significant in the global budget, play only a minor role in driving changes in COS concentration over most vegetated regions in the absence of fires. The NOAA-ESRL global monitoring network provides a multiannual record of COS at 13 background atmospheric sampling sites. Atmospheric sampling programs have collected approximately 8000 point measurements of COS and CO_2 concentration from aircraft in the free troposphere and atmospheric boundary layer over vegetated areas per year. Some measurements of COS concentration are now being obtained from the ACE satellite, and there are prospects for expanded sampling of this trace gas from satellite and surface locations. The goal of this work is to develop a modeling framework for interpreting these data and to illustrate what COS measurements might tell us about disentangling component processes of the carbon cycle, particularly separating the photosynthetic and respiratory terms that are confounded in the measurement of CO_2 fluxes and concentrations.

2. Methods

2.1. Transport Model

[3] We chose to use the Parameterized Chemical Transport Model (PCTM, http://code916.gsfc.nasa.gov/Public/Modelling/pctm/pctm.html) and meteorology from NASA's GEOS-4 model (http://gmao.gsfc.nasa.gov/systems/geos4) to simulate the 3-D variation in the concentration of CO_2 and COS in the global atmosphere given gridded fields of the surface sources and sinks of COS and CO_2. Simulations were run for the years 2002–2005. Since the GEOS-4 reanalysis provides a reconstruction of the motion of the atmosphere through actual time, the modeled concentrations should be comparable to samples taken at specific times and places in the atmosphere. *Kawa et al.* [2004] showed that PCTM exhibits considerable skill in matching synoptic and seasonal variation in CO_2 concentration at sites where continuous measurements of CO_2 were available, and PCTM simulations have been widely used for inversions and data assimilation of carbon cycle processes [*Hammerling et al.*, 2012; *Lokupitiya et al.*, 2008; *Parazoo et al.*, 2011].

[4] The monthly averaged observed concentrations were compared with monthly averaged simulated concentrations from a range of PCTM simulations driven by alternative source and sink estimates (Table 1). All PCTM simulations were driven by biomass burning emissions scaled in space and time by the global fire emissions database (GFED) global inventory [*van der Werf et al.*, 2003], anthropogenic fluxes from the Kettle inventory [*Kettle et al.*, 2002], and an atmospheric OH sink estimated using GEOS-4 monthly mean temperature and zonal mean OH [*Bian et al.*, 2007]. For terrestrial and ocean fluxes, the PCTM simulations used the Kettle inventory or the new flux estimates described below.

2.2. Global Surface Fluxes

[5] The gridded flux inventory of COS presented by *Kettle et al.* [2002] is the starting point for this modeling study (Table 1). Simulations with PCTM using these sources and sinks match the background concentration of COS fairly well, but as shown in Figure 1, seasonal variation of COS at continental sites is too small. This is not surprising since Kesselmeier and co-workers have suggested a substantially larger uptake by leaves [*Sandoval-Soto et al.*, 2005] and soils [*Van Diest and Kesselmeier*, 2008 and loc. cit.] based on chamber studies. *Protoschill-Krebs et al.* [1996] identified that the biochemical mechanism responsible for uptake of COS by leaves and soils is a hydrolysis reaction catalyzed by the enzyme carbonic anhydrase leading to production of H_2S and CO_2. This new information was used previously to construct a regional model of COS flux [*Campbell et al.*,

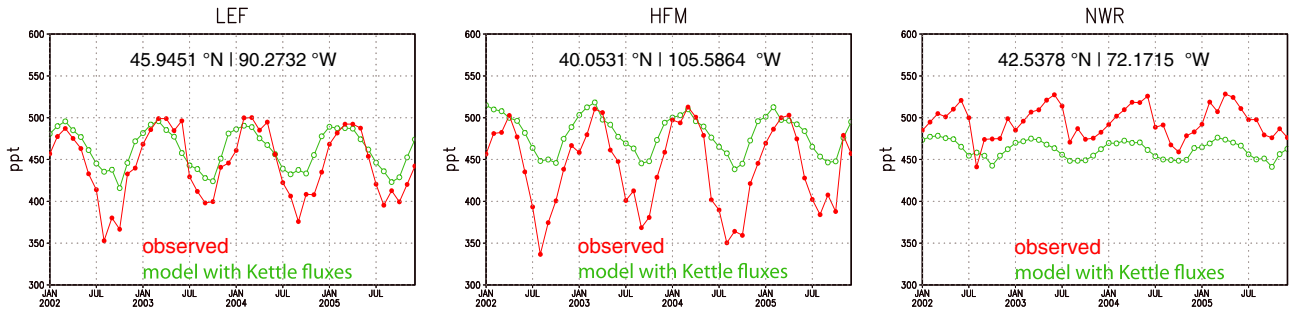

Figure 1. Observed (red) COS monthly mean concentrations at the WLEF tower in Wisconsin, Harvard Forest and Niwot Ridge, in comparison with simulations (green) using the benchmark sources and sinks given by *Kettle et al.* [2002] and a biomass burning source. Data were obtained from NOAA-ESRL global monitoring network [*Montzka et al.*, 2007].

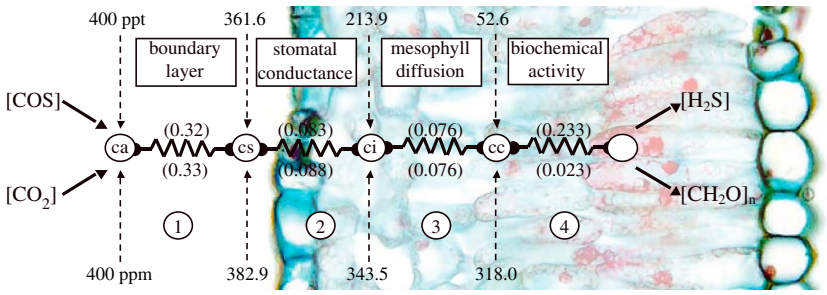

Figure 2. Resistance analog model of CO_2 and COS uptake. Numbers in parentheses are conductance values (mol m^{-2} s^{-1}) corresponding to the numbered key: (1) Boundary layer conductance, g_b. (2) Stomatal conductance, g_s. (3) Mesophyll conductance, g_i. (4) Biochemical rate constant used approximate photosynthetic CO_2 uptake by Rubisco or the reaction of COS with carbonic anhydrase as a linear function of c_c. In this case, COS uptake is 12.6 pmol m^{-2} s^{-1} and that of CO_2 is 5.6 μmol m^{-2} s^{-1}.

2008], but to our knowledge has not previously been used to construct a model for COS exchange by plants and soil that could be run globally. We chose to use the carbon cycle model SiB3 [*Baker et al*., 2008; *Baker et al*., 2007] for this purpose.

2.3. COS Leaf Uptake

[6] CO_2 and COS take the same pathway for diffusion from the atmosphere to the site of reaction. COS is consumed inside leaf cells by the enzyme carbonic anhydrase (CA), which is colocated in the chloroplasts of leaves with Rubisco—the enzyme that consumes CO_2 in the first step of photosynthesis. We assume that COS uptake is unidirectional as shown in Figure 2. Models for the diffusion of CO_2 into leaves and its consumption by photosynthesis are well developed and are more or less standardized in land surface models [*Bonan*, 2008]. Our goal here is to extend one of these models [*Sellers et al*., 1996a] to simulate the diffusion and uptake of COS. Water vapor fluxes are normally used to evaluate the exchange of gas between the leaf interior and the surrounding air. The stomatal pore and leaf boundary layer impose resistances to diffusion (or alternatively conductances = 1/resistance), and these are modeled using an empirical relationship [*Ball et al*., 1987]. The diffusive resistances of CO_2 and COS are framed in reference to that of H_2O vapor. The greater mass and larger cross section of COS restricts its diffusion relative to H_2O in the stomatal pore by a factor of 1.94 and in the laminar boundary layer by 1.56 [*Seibt et al*., 2010; *Stimler et al*., 2010], whereas analogous values for CO_2 are 1.6 and 1.4 [*Bonan*, 2008]. Thus, gas phase diffusion of COS is about 20% slower than CO_2. Liquid phase and aerodynamic conductances to COS were assumed to be equal to that for CO_2. Once COS has diffused into the leaf cell, it is hydrolyzed in a reaction catalyzed by CA, at a rate, J_{COS}, determined by its partial pressure in the choloplast, $p\mathrm{COS}_c = [\mathrm{COS}]_c{}^*P$, where $[\mathrm{COS}]_c$ is the COS mole fraction in the chloroplast, and P is the total pressure (Pa). In principle, this could be modeled using Michaelis-Menten kinetics:

$$J_{\mathrm{COS}} = p\mathrm{COS}_c \frac{vm}{k_{1/2} + p\mathrm{COS}_c} \quad (1)$$

where vm is the maximum reaction rate, and $k_{1/2}$ is the half-saturation constant. However, because $p\mathrm{COS}_c$ (10–20 μPa) is typically much less than $k_{1/2}$ (200–4000 Pa), this reaction can be approximated as a first order process:

$$J_{\mathrm{COS}} = p\mathrm{COS}_c{}^*v_0 \quad (2)$$

where $v_0 = vm/k_{1/2}$ is an effective first order rate constant (mol m^{-2} s^{-1} Pa^{-1}) that determines the rate of uptake of COS from the intercellular air spaces per leaf area. Since CO_2 is an alternative substrate for CA and COS for Rubisco, they can act as competitive inhibitors, but this effect is negligible at the relative concentrations of COS and CO_2 present in a leaf under ambient conditions. The apparent activity for COS uptake is a function of both the amount of CA enzyme and where it is located relative to the intercellular air spaces—a factor that introduces a finite mesophyll conductance. At the present time, we have little information on either of these, but independent studies indicate that both CA activity [*Badger and Price*, 1994] and mesophyll conductance [*Evans et al*., 1994] tend to scale with the photosynthetic capacity or the *Vmax* (μmol m^{-2} s^{-1}) of Rubisco present in the leaf. We therefore assume that both the mesophyll conductance and v_0 are proportional to the *Vmax* of Rubisco. In addition, we note that v_0/P has the dimensions of—and functions in a way analogous to—a conductance for COS uptake with a COS concentration of zero at the terminus. Hence, the two processes, mesophyll conductance and CA activity, can be combined into a single apparent conductance for COS uptake from the intercellular airspaces that is proportional to *Vmax*, i.e., $g_{\mathrm{COS}} = \alpha{}^*Vmax$. Thus,

$$F_{\mathrm{COS}} = [\mathrm{COS}]_a{}^*[1.94/g_{sw} + 1.56/g_{bw} + 1.0/g_{\mathrm{COS}}]^{-1} \quad (3)$$

where F_{COS} is the flux of COS uptake, $[\mathrm{COS}]_a$ is the COS mole fraction in the bulk air, and the terms in brackets represent the series conductance of the leaf system for COS calculated from the respective conductances to water vapor simulated by the model (Figure 2). The effective *Vmax* of Rubisco in the model is modulated by temperature and the presences of high temperature or water stress. We assume that these affect g_{COS} similarly.

[7] We used gas exchange observations of simultaneous measurements of COS and CO_2 uptake [*Stimler et al*., 2012; *Stimler et al*., 2010] to calibrate the parameter α used in the model to scale g_{COS} to *Vmax*. First, the *Vmax* parameter was fit individually to each gas exchange experiment (36 with C3 and 7 with C4 leaves, each consisting of 3–12 separate

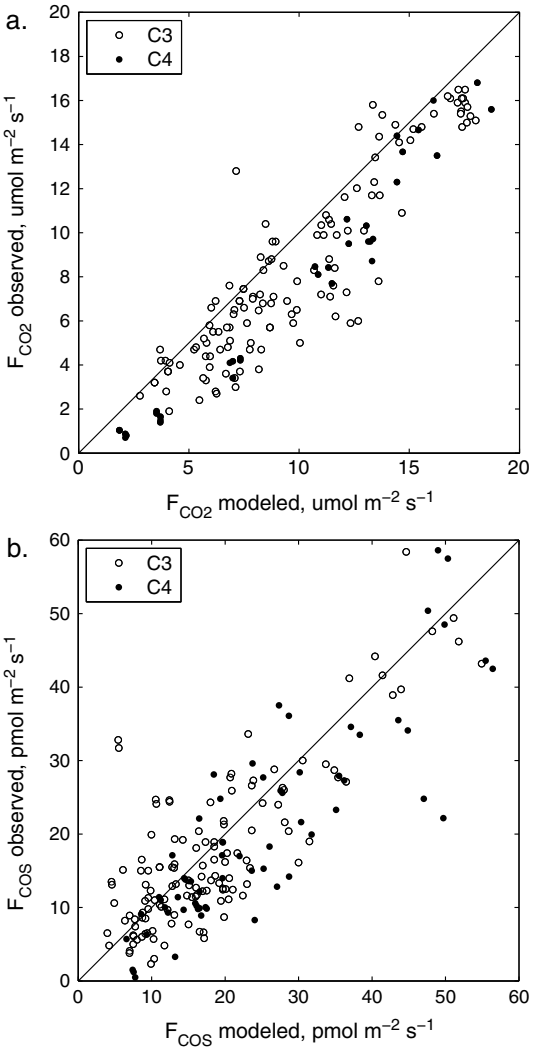

Figure 3. Comparison of modeled and observed COS and CO_2 fluxes from experiments [*Stimler et al*., 2010, 2012]. (a) CO_2 fluxes; (b) COS fluxes.

measurements with variation in light, temperature, [CO_2], or [COS]; $n = 200$ C3 and 80 C4 observations). Next, the photosynthesis submodel of SiB3 was used to simulate F_{CO2} and F_{COS} using the observed environmental conditions, and a single value of α was fit to constrain the slope of a Type II regression of F_{COS} between observations and the model to the 1:1 line, yielding an estimate of $\alpha \approx 1200$ for all C3 and 13,000 for all C4 species (Figure 3b). We note that while the fit of *Vmax* results in a fairly good match of F_{CO2} (Figure 3a) with observations ($r^2 = 0.87$) and a small bias (~10% low), the value of α is not very well constrained by the data ($r^2 = 0.63$) for the combined data set. Nevertheless, very good linear relationships were obtained when subsets of the data from experiments from a single plant were examined, indicating that much of the variability comes from plant to plant variability in CA activity and/or mesophyll conductance. The value of g_{COS} for C3 leaves is similar to estimates of the mesophyll conductance for CO_2 in other studies [*Evans et al*., 1994]. Analysis of the control of F_{COS} ($\partial F_{COS}/F_{COS}$)/($\partial g_{COS}/g_{COS} = 0.51$ and 0.26 for C3 and C4 plants, respectively) indicating that uptake by C3 plants is more sensitive to the value of g_{COS} than C4 plants or that C4 plants are more strongly controlled by stomatal conductance. The higher value of α for C4 plants reflects that fact that they have similar rates of COS uptake and lower content of Rubisco than C3 plants [for a discussion, see *Stimler et al.,* 2011]. The global simulations were conducted with an older calibration than that reported here. The original calibration underestimated uptake by C4 species. We determined that the current calibration would yield about 10% larger total COS flux with the calibration data set. It was not practical to repeat global simulations for small changes in calibration coefficients. On the other hand, it makes no sense to present obsolete calibration information.

2.4. COS Soil Uptake

[8] The enzyme carbonic anhydrase also occurs in soil organisms [*Seibt et al*., 2006; *Wingate et al*., 2008]. Thus, COS that diffuses into the soil can also be hydrolized. The rate is a function of the activity of CA, the temperature of the soil, its porosity, and water content [*Van Diest and Kesselmeier*, 2008]. However, lacking information on CA activity of soils globally, we opted to use the observation that soil uptake of COS is proportional to CO_2 production by soil respiration [*Yi et al*., 2007]. This is plausible as CA activity is likely to vary with the microbial biomass in the soil and with temperature and water availability. Therefore, we modeled the soil COS flux (J_{soil}) as a function of heterotropic respiration (R_h):

$$J_{soil} = k_{soil} * f(\theta) * R_h \quad (4)$$

where k_{soil} is a proportionality constant (0.00012 mol COS/mol CO_2) that relates the COS flux with R_h, with additional control by the fraction of water filled pore space (θ), which limits diffusion of COS [*Van Diest and Kesselmeier*, 2008]. The function $f(\theta)$ forces J_{soil} to fall more quickly with soil moisture; it reaches a maximum of 1 at when $\theta = 0.3$ (low soil moisture and high aeration) and falls to a minimum of 0 when $\theta = 1$ (complete saturation). In SiB3, R_h is modeled separately for each soil layer as a function of root density, soil moisture and temperature, and a rate constant that is adjusted such that the seasonal total of CO_2 release in heterotrophic respiration is equal to the seasonal total of net primary production [see *Baker et al*., 2007; *Denning et al*., 1996]. We calculated COS uptake according to equation (4) for each soil layer separately. Some upland soils can be a source of COS [*Melillo and Steudler*, 1989]. No soil source was included in this study.

2.5. Ecosystem Simulations

[9] The Simple Biosphere Model (SiB) was introduced [*Sellers et al*., 1986] as a lower boundary for Atmospheric General Circulation Models (AGCMs), albeit with a level of ecophysiological realism that makes SiB useful to ecologists as well. SiB is categorized as a so-called "enzyme kinetic" model that follows *Farquhar et al.* [1980], *Collatz et al*. [1991, 1992] and *Sellers et al*. [1992] in the calculation of photosynthetic processes. SiB was reformulated in 1996 to include satellite data to constrain simulated phenology [*Sellers et al*., 1996a; *Sellers et al*., 1996b] and has been since modified to include a prognostic canopy air space [*Baker et al*., 2003; *Vidale and Stockli*, 2005], multiple physiology types (i.e., colocation of C3 and C4 grasses; *Hanan et al*.

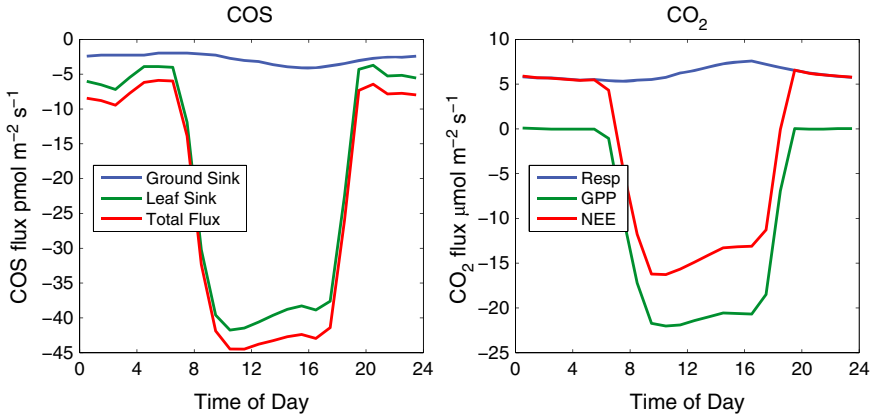

Figure 4. Diel variation in CO_2 and COS exchange simulated at the Km 83 site near Santarem, Brazil. Note that daytime GPP and leaf COS uptake are parallel. COS uptake by the soil is probably not correlated with GPP (although it is in current model), and some leaf and soil uptake continues at night owing to incomplete stomatal closure.

[2005]) and modifications that improve performance in tropical and sub-tropical regions [*Baker et al*., 2008, *Baker et al*., 2013]. We call the current version of the model SiB3.

[10] SiB3 calculates photosynthesis for a unit ground area and scales from leaf- to canopy-scale following *Sellers* [1985] and *Sellers et al*. [1992, 1996a]. Calculation of transpiration and sensible heat fluxes couple the Bowen ratio to the calculation of stomatal conductance and remotely observed values of fraction of Photosynthetically Active Radiation (fPAR) absorbed by the canopy. SiB3 does not simulate processes explicitly for sunlit and shaded leaves [i.e., *de Pury and Farquhar*, 1997; *Wang and Leuning*, 1998], but the scaling method is robust enough that SiB3 performs strongly in inter-model comparison projects when evaluated against formulations that are both simpler and more complex [*Schwalm et al*., 2010].

[11] Simulations were conducted with SiB3-COS over a range of ecosystems using surface meteorology derived from reanalysis (NCEP-2; *Kalnay et al*. [1996]; *Kanamitsu et al*. [2002]) and vegetation dynamics and density derived from satellite observations (GIMMSg normalized difference vegetation index; *Brown et al*. [2004]; *Pinzon et al*. [2005]; *Tucker et al*. [2005]). Figure 4 shows typical diurnal courses of CO_2 and COS exchange for an Amazon forest ecosystem near the end of the dry season. SiB3 has demonstrated a fidelity to observed fluxes of carbon, water, and energy at this site (KM83) on both diurnal and seasonal scales [*Baker et al*., 2008; *Baker et al*., 2013]. These simulations do not specify the COS leaf fluxes as a fixed ratio to the CO_2 leaf fluxes—as has been done previously [*Campbell et al*., 2008; *Sandoval-Soto et al*., 2005; *Suntharalingam et al*., 2008]. Instead, these new flux estimates are calculated by the mechanistic parameterization based on environmental conditions, stomatal conductance, and physiological stress as simulated by SiB.

2.6. Observations

[12] NOAA/ESRL measurements of COS and CO_2 have been regularly measured from samples collected from global surface sites since 2000 [*Montzka et al*., 2007]. We analyzed measurements from 12 sites including 10 background sites (SPO, South Pole; CGO, Cape Grim, Australia; SMO, American Samoa; MLO, Mauna Loa, United States; Cape Kumukahi, United States; Niwot Ridge, United States; BRW, Barrow, United States; ALT, Alert, Canada; MHD, Mace Head, Ireland; SUM, Summit, Greenland; PSA, Palmer Station, Antarctica; TDF, Tierra Del Fuego, Argentina; and THD, Trinidad Head, United States) and two continental sites (LEF, Wisconsin, United States and HFM, Harvard Forest, United States). Results were discarded when paired flasks disagreed by more than 6.3 ppt, accounting for 15% of all samples collected. Carbonyl sulfide data from this network are available on line at: ftp://ftp.cmdl.noaa.gov/hats/carbonyl%20sulfide/.

[13] COS measurements were made during INTEX-NA (North America, July/August 2004) and TC4 (tropical Latin and South America, July/August 2007) from whole air samples, collected in specially prepared evacuated 2 L stainless steel canisters, filled every 1 to 5 min [*Blake et al*., 2008]. The measurement precision for COS during TC4 was better than 1% with 5% accuracy and a detection limit better than 20 ppt. The gas was always present above the detection limit. In situ observations of atmospheric CO_2 ($\pm$0.25 ppm-molar uncertainty) were made with a modified Li-Cor model 6252 nondispersive infrared analyzer at a frequency of 1 Hz [*Vay et al*., 2003]. In-flight calibrations for CO_2 were performed every 15 min using standards traceable to the WMO Central Laboratory at NOAA/ESRL.

3. Results and Discussion

3.1. Revised Ocean Source

[14] SiB3-COS was used to simulate global fluxes of CO_2 and COS hourly at $1^\circ \times 1^\circ$ resolution for 2002–2005. However, as shown in Table 1, the total land sink was approximately threefold larger in the SiB3 based simulations than that originally estimated by the Kettle inventory [*Kettle et al*., 2002]. This upward revision to the global plant sink is within the range of the most recent global estimates based on plant chamber [*Sandoval-Soto et al*., 2005; *Stimler et al*., 2010] and atmospheric analysis studies [*Campbell et al*., 2008; *Montzka et al*., 2007; *Suntharalingam et al*., 2008]. An initial PCTM simulation was run with the new SiB plant and soil sinks, but using the Kettle inventory data for direct and indirect

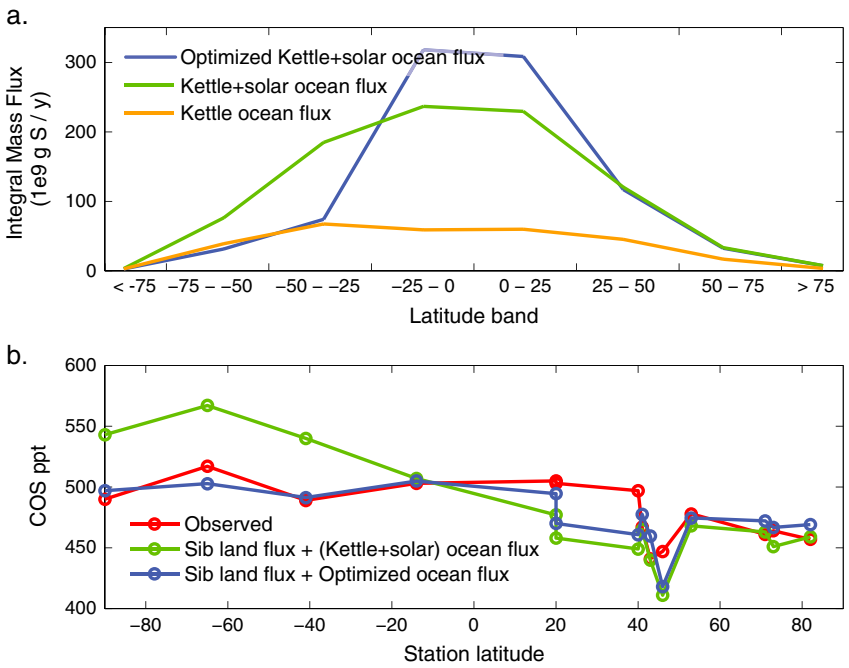

Figure 5. The original and optimized latitudinal distribution of the ocean source (direct and indirect) used in this study. (a) Mass fluxes for each latitude band, showing original *Kettle et al.*, 2002 flux, Kettle and new ocean source (proportional to monthly gridded solar insolation) to balance increased land uptake, and optimized redistribution of this combined ocean source to match observations. (b) Comparison of new land and ocean fluxes in this paper with surface station annual mean observations. Sites are as follows: ALT, SUM, BRW, MHD, LEF, HFM, THD, NWR, MLO, KUM, SMO, CGO, PSA, and SPO. Data were obtained from NOAA-ESRL global monitoring network [*Montzka et al.*, 2007].

sources from anthropogenic activities and ocean processes and sinks due to biomass burning and OH oxidation (Figure 1). This PCTM simulation resulted in large errors in the latitudinal variation in the atmospheric COS concentration (Figure 4).

[15] To reduce the error between COS simulations and observations, it was necessary to make an adjustment in the modeled fluxes. Atmospheric observations during this period do not show strong long-term trends over the years 2000 to 2005 [*Montzka et al.*, 2007]. Given these relatively steady-state conditions, the sources and sinks must be balanced in the model. While the Kettle inventory sources and sinks are balanced, our upward revision to the plant and soil sinks requires an adjustment in the other fluxes of 727 Gg S y^{-1} to balance the budget. The adjustment could require a reduction in the sinks or an increase in the sources or some combination of the two. Since the sinks other than plant and soil sinks are small, the adjustment should be applied to increase the sources. The anthropogenic source has relatively little seasonality, so that adjustment of this source is unlikely to correct the model error associated with seasonal amplitude. The remaining sources are from the ocean and biomass burning. Adjustments to these large sources provide one starting point for simulating COS with a balanced budget.

[16] We initialize a simple inverse analysis with a biomass burning source at the upper end of the reported range (136 Gg S y^{-1}) and a missing ocean source that balances the residual of the budget (600 Gg S y^{-1}). Following *Cutter et al.* [2004], we distributed the missing ocean source in space according to the incident solar flux (Figure 5a). We then used a simple inversion approach to optimize the latitudinal distribution of the ocean source (direct and indirect) in order to obtain a better fit to the data while maintaining mass balance. The full set of surface boundary conditions, including the solar-distributed oceanic source of COS, was run in PCTM to simulate concentrations of COS at each of 13 NOAA atmospheric background sites. In addition, the baseline plus a perturbation of the total ocean source was run for each of six latitudinal bands, with the total quantity of the perturbation recorded. A linear solver was then used to adjust weights applied to each latitudinal band to minimize the discrepancy with the observations subject to the constraint that the total ocean flux remained constant. The solver makes the assumption that changes in [COS] are linearly proportional to changes in COS flux. The form of the solver was to minimize $\Sigma(Cx - d)^2$ subject to $a^{\mathrm{T}}x = 0$, where x is the unknown amount of perturbation to the ocean source (default = 0), C is the (13 × 6) matrix of simulated differences in [COS] at observation sites between each perturbation and the baseline run, d is the vector of differences between the observed [COS] and the baseline simulated [COS], and a is the vector containing the total mass flux for each perturbation. By setting the constraint to zero, any perturbation in one band must be balanced by a compensating perturbation in other bands. The resulting distribution of this optimized ocean COS source is concentrated in the tropics (Figure 5a) and has substantially lower intensities in the higher latitudes of both hemispheres to match observations (Figure 5b). This concentration of the missing source in the tropics is consistent with the results of another global analysis that was based on an empirical model of

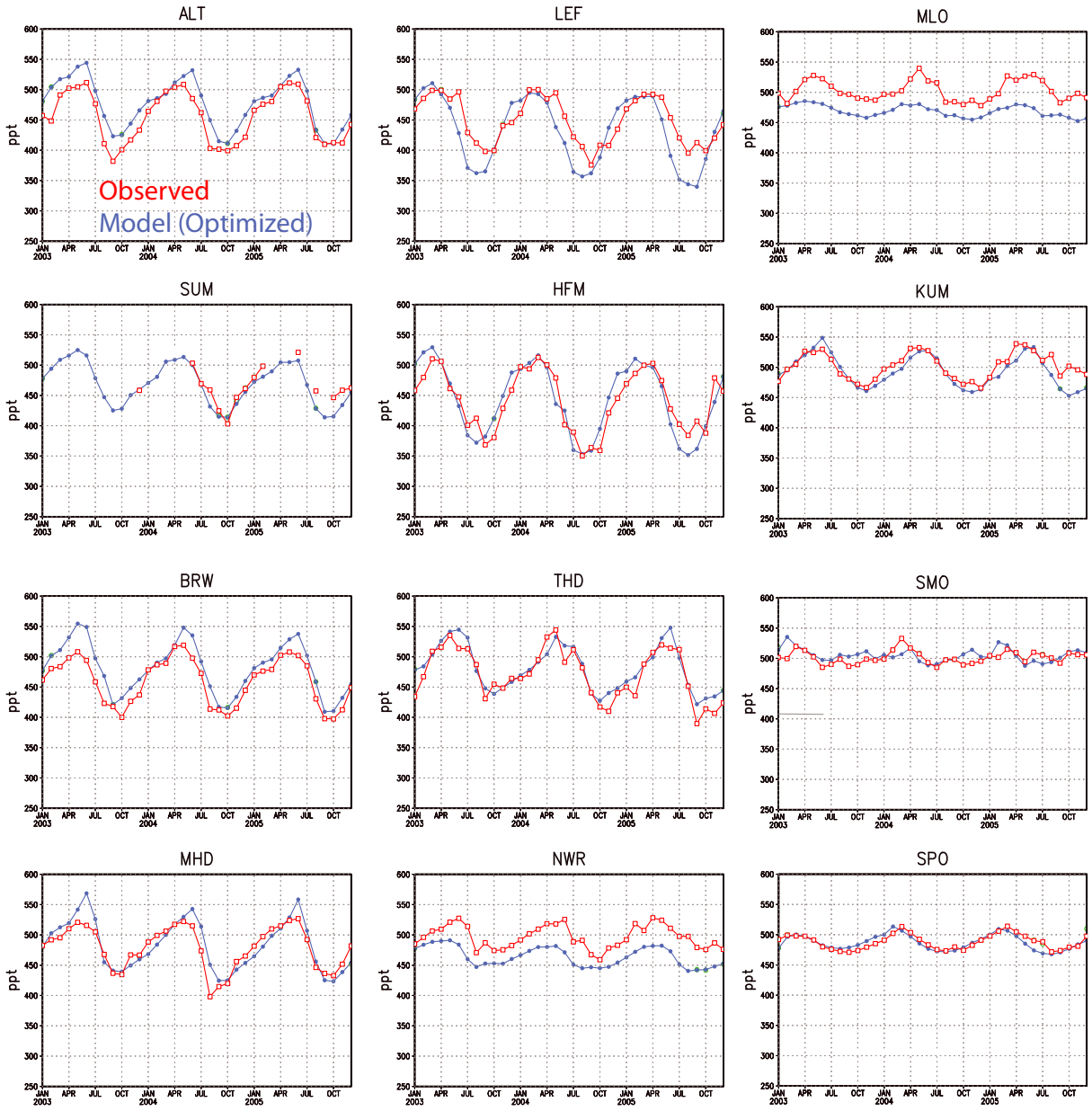

Figure 6. Observations (red) of seasonal variation in COS concentration at the NOAA background atmosphere sampling stations, in comparison with simulations (blue) using revised sources and sinks developed in this paper. Data were obtained from NOAA-ESRL global monitoring network [*Montzka et al.*, 2007].

terrestrial surface fluxes, which in contrast to the present study made the assumption that the missing source is distributed evenly across oceans and land [*Suntharalingam et al.*, 2008].

3.2. Validation: Seasonal Cycle at GMD Sites

[17] A reasonable fit for the COS concentrations was obtained at the background stations (Figure 6) and the continental sites, and the new boundary conditions presented here better approximate the observations than the prior Kettle boundary conditions (Figure 1). The largest errors are now at Mauna Loa, Hawaii (MLO) and Niwot Ridge, Colorado (NWR). The atmospheric simulations predict substantial longitudinal gradients (~50 ppt) in surface concentration across the tropical Pacific and a similar longitudinal drawdown in the upper troposphere over the continents (data not shown).

3.3. Validation: Relative Seasonal Amplitude of COS and CO_2

[18] Previous work [*Montzka et al.*, 2007] has observed a strong correlation between the normalized seasonal amplitude of COS and CO_2 at NOAA Northern Hemisphere background sites ($r^2 = 0.9$; slope $= 6 \pm 1$). Here we report a similar relationship for the normalized seasonal amplitude of COS and CO_2 simulated by PCTM (Figure 7; $r^2 = 0.97$; slope $= 3.6$) in which the CO_2 simulations were only driven by SiB global fluxes of net ecosystem exchange (no ocean or anthropogenic fluxes). The similar correlation between the seasonal cycles indicates

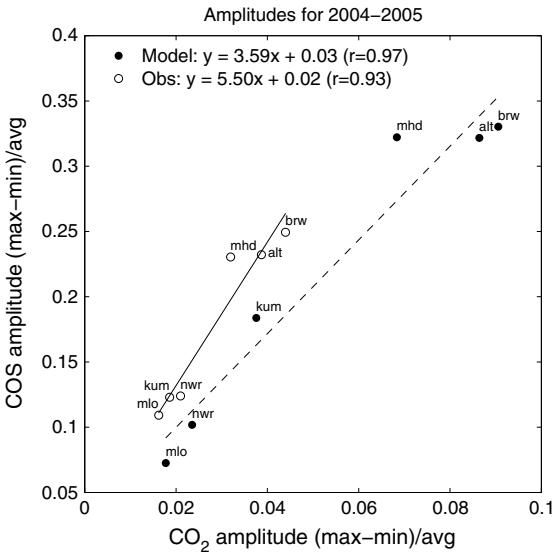

Figure 7. Simulated seasonal amplitude of COS at background sites versus seasonal amplitude of CO_2, in reference to observed seasonal amplitudes.

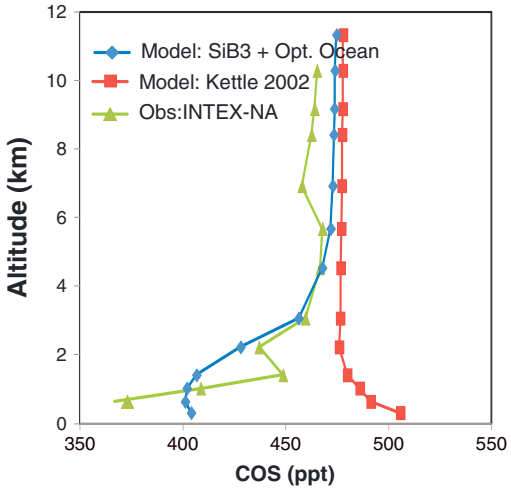

Figure 9. The monthly mean profile simulated by PCTM over Illinois and Indiana in July–August 2004 compared to the mean of flask samples taken by the INTEX-NA campaign.

that the coupling between the two global cycles in the model is a reasonable approximation to the real world. However, the substantially larger seasonal cycles in the simulations indicates that there is a problem with the model representation of both cycles. Possibilities include the following: (a) that GPP is over-estimated, (b) that the seasonal cycle of GPP is exaggerated, or (c) that meridional transport in PCTM is over estimated [see *Parazoo et al.*, 2011].

3.4. Validation: Vertical and Spatial Gradients

[19] The strong surface uptake simulated in the present study results in a strong drawdown of the atmospheric boundary layer concentrations relative to the concentrations in the free troposphere over land but not over the ocean. There are many observations of these vertical gradients from atmospheric sampling campaigns. Figure 8 shows data for two vertical profiles from the NASA-TC^4 mission in the Columbian Amazon on 8 August 2007 [*Toon et al.*, 2010].

At one point, the plane dropped down into the boundary layer over the ocean where there was a small increase in COS concentration. In contrast in a second profile over the central Amazon, the COS concentration dropped abruptly by 70 ppt and CO_2 by 6 ppm. The latter profile is very similar to that simulated for the monthly mean profile at that grid box in PCTM in previous years.

[20] Figure 9 shows the mean vertical profile for the Mid-continent of North America during the active growing season from the INTEX-NA mission in July and August of 2004 [*Blake et al.*, 2008; *Campbell et al.*, 2008]. The enhanced uptake from the SiB model provides an improved match for the observed INTEX-NA drawdown relative to the simulations based on the much smaller sinks in the Kettle inventory. The simulations based on the Kettle input show a surface enhancement rather than drawdown, because the anthropogenic fluxes are larger than the Kettle plant and soil fluxes in the Mid-continent region. These preliminary tests provide validation of the new land flux used in the current model and indicate that a strong continental source is unlikely.

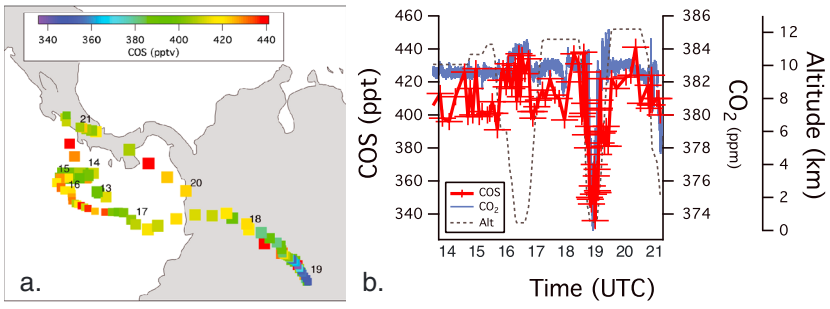

Figure 8. CO_2 and COS concentration measured in one flight leg (8 August 2007) of the TC^4 campaign. (a) COS concentration along the flight path into the Columbian Amazon. COS is depicted by marker color (warmer colors is higher concentration) and flight altitude is depicted by marker size (larger size is lower altitude). (b) Time series of CO_2, COS and altitude for the flight depicted in Figure 8a. Low altitude passes include collection in the marine boundary layer (UTC 16 h) and the continental boundary layer (UTC 19 h).

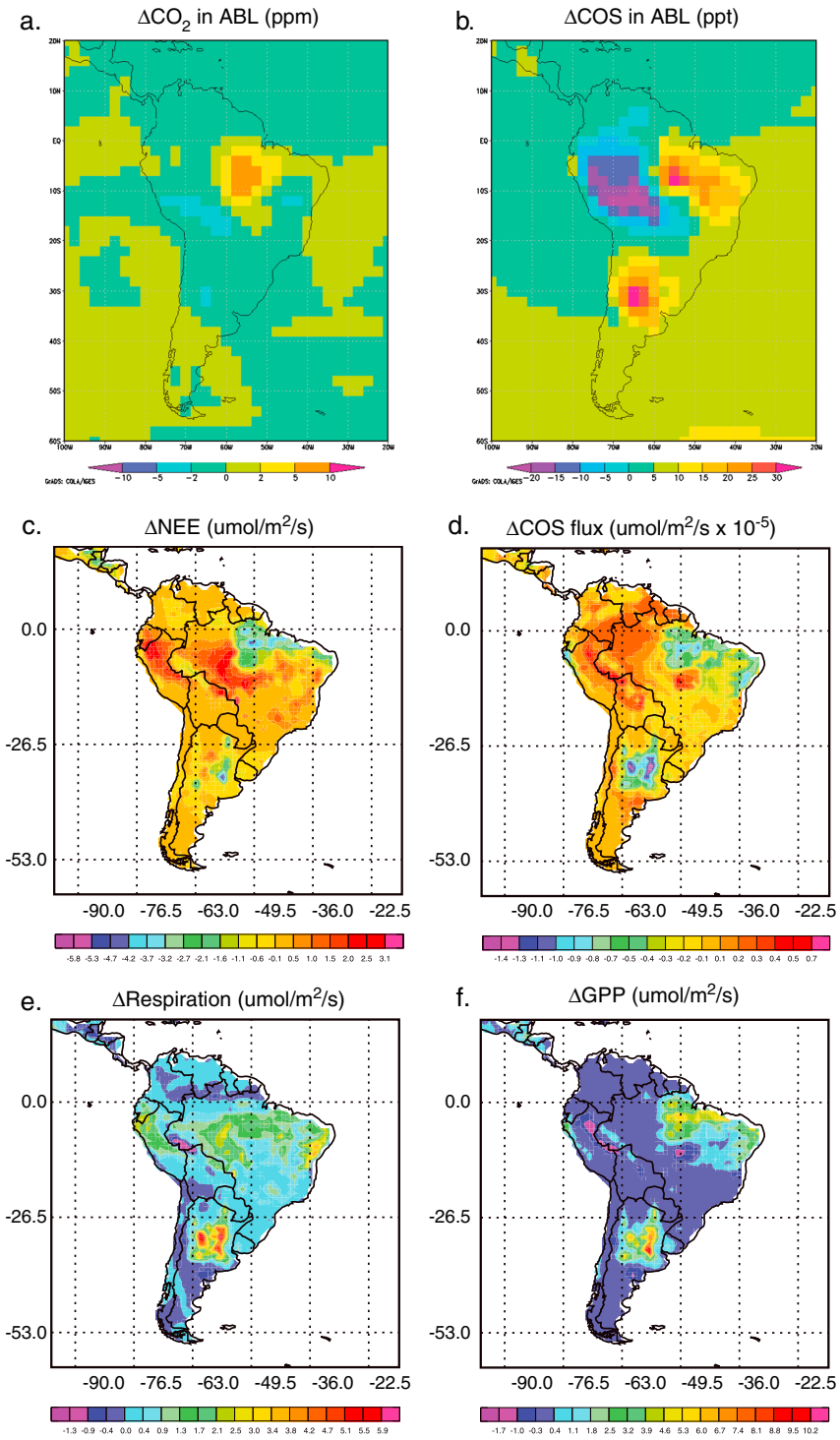

Figure 10. Maps illustrating the use of COS as a diagnostic between different land surface model soil hydrology implementations. Maps show the difference in (a–b) ABL concentration and (c–f) surface fluxes for CO_2 and COS for different parameterizations (new-old) over South America in January 2005. Positive values in Figures 10a and 10b indicate increased drawdown indicative of increased net uptake in the new parameterization; negative values in Figures 10c–10f indicate increased flux. An area of enhanced CO_2 drawdown (5–10 ppm) in the ABL is seen over the Eastern Amazon, with corresponding enhanced COS drawdown (20–40 ppt) over the same area. Another area of COS drawdown is seen over an area south of the Amazon, but with no corresponding area of enhanced CO_2 drawdown. See the text for interpretation.

4. Outlook

4.1. Using Differential Patterns in COS and CO_2 Drawdown to Diagnose Carbon Cycle Processes

[21] We designed a simulation experiment to examine if differential responses of photosynthesis and respiration could be seen from hypothetical atmospheric measurements of COS and CO_2. We conducted two global simulations each with a different implementation of soil hydrology and water stress. The original SiB version was known from comparisons with ecosystem scale measurements at an eddy correlation tower in the Eastern Amazon near Santaram to over-estimate drought stress. In the original simulation, the canopy developed severe water stress near the end of the dry season, yet this was not seen in the eddy correlation studies conducted in the forest. To correct this problem, the soil was made deeper, and root-mediated redistribution of soil water was implemented in a new version of the SiB model [*Baker et al*., 2008]. This modification reduced the simulated inhibition of photosynthesis and enhanced COS uptake by eliminating soil water stress. The two different model implementations were run globally, including atmospheric transport simulated by PCTM. Figure 10 shows plots of the difference in the simulated mid-boundary layer concentration drawdown for CO_2 and COS over South America. The model with the improved hydrology showed stronger drawdown of both COS and CO_2 in the ABL over Eastern Amazon, which was consistent with the difference seen in site level simulations. In this region, maps of the fluxes coincided with the simulated atmospheric tracer anomalies. Examination of the simulated fluxes showed that photosynthesis and COS uptake were enhanced by the improved soil hydrology. However, respiration was not greatly affected, and consequently there was an enhanced drawdown of CO_2 in addition to COS.

[22] The changed soil moisture parameterization also had strong effects on the concentrations of COS and CO_2 over other areas of South America, but unlike the Eastern Amazon, the two species did not change in tandem. In particular, note the enhanced COS drawdown to the south of the Amazon basin that was *not* accompanied by an enhanced CO_2 drawdown. Inspection of the simulated fluxes in that region indicated that photosynthesis was indeed stimulated in this area, but in contrast to the forest ecosystem to the north, respiration was also stimulated, neutralizing changes in the net ecosystem CO_2 exchange. This region is a grassland ecosystem with shallower soils and more roots near the surface. Apparently the new hydrology resulted in more soil moisture in surface layers that stimulated both photosynthesis and respiration. Thus, there was no net effect on CO_2 flux, but a stimulation of COS uptake. Another area in the Western Amazon shows decreased COS drawdown with little or no CO_2 effect. The change in hydrology depressed both photosynthesis, COS uptake, and respiration in this region. These simulations provide interesting examples of differential responses of photosynthesis and respiration that have clearly interpretable manifestations in the comparative drawdown of CO_2 and COS. Clearly, COS data could provide process level insights additional to those we could distinguish from only looking at the CO_2 concentration. Some deficiencies in the present modeling system should also be noted. A more mechanistic representation of soil uptake of COS is needed, and the treatment of radiation and turbulent transport in the canopy can certainly be improved. However, there are very few direct measurements of COS flux from ecosystems or soils with which to calibrate or falsify these models. Hopefully, this will change with the availability of new instrumentation for measurement of COS [*Asaf et al*., 2013].

[23] In summary, we demonstrated using a simulation experiment that COS data could provide additional information on the separate responses of photosynthesis and respiration to environmental forcing. The simulations presented here indicate that measurement of COS could provide improved constraints on 4-D data assimilation of carbon cycle processes.

[24] **Acknowledgments.** We gratefully acknowledge George Wolf and Orrick, Herrington & Sutcliffe LLP for providing a meeting space to develop this work and Mohammad Abu-Naser for helping in the preparation of figures. This research was supported in part by the NASA Earth Science Program and the Office of Science (BER), U. S. Department of Energy. This research also had substantial contributions that were conducted without grant support and reflect the generosity of our colleagues and home institutions.

References

Asaf, D., E. Rotenberg, F. Tatarinov, U. Dicken, S. A. Montzka, and D. Yakir (2013), Ecosystem photosynthesis inferred from measurements of carbonyl sulphide flux, *Nat. Geosci.*, *6*(3), 1–5, doi:10.1038/ngeo1730.

Badger, M. R., and G. D. Price (1994), The role of carbonic-anhydrase in photosynthesis, *Annu. Rev. Plant Physiol.*, *45*, 369–392.

Baker, I., A. S. Denning, N. Hanan, L. Prihodko, M. Uliasz, P. L. Vidale, K. Davis, and P. Bakwin (2003), Simulated and observed fluxes of sensible and latent heat and CO_2 at the WLEF-TV tower using SiB2.5, *Global Change Biol.*, *9*(9), 1262–1277.

Baker, I. T., A. S. Denning, L. Prihodko, K. Schaefer, J. A. Berry, G. J. Collatz, N. S. Suits, R. Stockli, A. Philpott, and O. Leonard (2007), Global Net ecosystem exchange (NEE) of CO_2, Oak Ridge National Laboratory Distributed Active Archive Center.

Baker, I. T., L. Prihodko, A. S. Denning, M. Goulden, S. Miller, and H. R. da Rocha (2008), Seasonal drought stress in the Amazon: Reconciling models and observations, *J. Geophys. Res.*, *113*, G00B01, doi:10.1029/2007JG000644.

Baker, I. T., et al. (2013), Surface ecophysiological behavior across vegetation and moisture gradients in tropical South America, *Agric. For. Meteorol.*, doi:10.1016/j.agrformet.2012.11.015, in press.

Ball, J. T., I. E. Woodrow, and J. A. Berry (1987), A model predicting stomatal conductance and its contribution to the control of photosynthesis under different environmental conditions, in *Progress in Photosynthesis Research*, vol. IV, edited by J. Biggins, pp. 221–234, Martinus Nijhof Publishers, Dordrecht.

Bian, H., M. Chin, S. R. Kawa, B. Duncan, A. Arellano, and P. Kasibhatla (2007), Sensitivity of global CO simulations to uncertainties in biomass burning sources, *J. Geophys. Res.*, *112*, D23308, doi:10.1029/2006JD008376.

Blake, N. J., et al. (2008), Carbonyl sulfide (OCS): Large-scale distributions over North America during INTEX-NA and relationship to CO(2), *J. Geophys. Res.*, *113*, D09S90, doi:10.1029/2007JD009163.

Blonquist, J. M., S. A. Montzka, J. W. Munger, D. Yakir, A. R. Desai, D. Dragoni, T. J. Griffis, R. K. Monson, R. L. Scott, and D. R. Bowling (2011), The potential of carbonyl sulfide as a proxy for gross primary production at flux tower sites, *J. Geophys. Res.*, *116*, G04019, doi:10.1029/2011JG001723.

Bonan, G. B. (2008), *Ecological Climatology: Concepts and Applications*, 2nd ed., xvi, 550 pp., Cambridge University Press, Cambridge; New York.

Brown, M. E., J. Pinzon, and C. J. Tucker (2004), New vegetation index dataset available to monitor global change, *Eos Trans. AGU*, *85*, 565.

Campbell, J. E., et al. (2008), Photosynthetic control of atmospheric carbonyl sulfide during the growing season, *Science*, *322*(5904), 1085–1088.

Collatz, G. J., J. T. Ball, C. Grivet, and J. A. Berry (1991), Physiological and environmental-regulation of stomatal conductance, photosynthesis and transpiration—A model that includes a laminar boundary-layer, *Agr. Forest Meteorol.*, *54*(2–4), 107–136.

Collatz, G. J., M. Ribas-Carbo, and J. A. Berry (1992), Coupled photosynthesis-stomatal conductance model for leaves of C4 plants, *Aust. J. Plant Physiol.*, *19*(5), 519–538.

Cutter, G. A., L. S. Cutter, and K. C. Filippino (2004), Sources and cycling of carbonyl sulfide in the Sargasso Sea, *Limnol. Oceanogr.*, *49*(2), 555–565.

Denning, A. S., G. J. Collatz, C. G. Zhang, D. A. Randall, J. A. Berry, P. J. Sellers, G. D. Colello, and D. A. Dazlich (1996), Simulations of terrestrial carbon metabolism and atmospheric CO_2 in a general circulation model .1. Surface carbon fluxes, *Tellus B*, *48*(4), 521–542.

Evans, J. R., S. Voncaemmerer, B. A. Setchell, and G. S. Hudson (1994), The relationship between CO_2 transfer conductance and leaf anatomy in transgenic tobacco with a reduced content of Rubisco, *Aust. J. Plant Physiol.*, *21*(4), 475–495.

Farquhar, G. D., S. V. Caemmerer, and J. A. Berry (1980), A biochemical-model of photosynthetic CO_2 assimilation in leaves of C-3 species, *Planta*, *149*(1), 78–90.

Hammerling, D. M., A. M. Michalak, C. O'Dell, and S. R. Kawa (2012), Global CO_2 distributions over land from the Greenhouse Gases Observing Satellite (GOSAT), *Geophys. Res. Lett.*, *39*, L08804, doi:10.1029/2012GL051203.

Hanan, N. P., J. A. Berry, S. B. Verma, E. A. Walter-Shea, A. E. Suyker, G. G. Burba, and A. S. Denning (2005), Testing a model of CO_2, water and energy exchange in Great Plains tallgrass prairie and wheat ecosystems, *Agr. Forest Meteorol.*, *131*(3–4), 162–179.

Kalnay, E., et al. (1996), The NCEP/NCAR 40-year reanalysis project, *Bull. Am. Meteorol. Soc.*, *77*(3), 437–471.

Kanamitsu, M., W. Ebisuzaki, J. Woollen, S. K. Yang, J. J. Hnilo, M. Fiorino, and G. L. Potter (2002), NCEP-DOE AMIP-II reanalysis (R-2), *Bull. Am. Meteorol. Soc.*, *83*(11), 1631–1643.

Kawa, S. R., D. J. Erickson, S. Pawson, and Z. Zhu (2004), Global CO_2 transport simulations using meteorological data from the NASA data assimilation system, *J. Geophys. Res.*, *109*, D18312, doi:10.1029/2004JD004554.

Kettle, A. J., U. Kuhn, M. von Hobe, J. Kesselmeier, and M. O. Andreae (2002), Global budget of atmospheric carbonyl sulfide: Temporal and spatial variations of the dominant sources and sinks, *J. Geophys. Res.*, *107*(D22), 4658, doi:10.1029/2002JD002187.

Lokupitiya, R. S., D. Zupanski, A. S. Denning, S. R. Kawa, K. R. Gurney, and M. Zupanski (2008), Estimation of global CO_2 fluxes at regional scale using the maximum likelihood ensemble filter, *J. Geophys. Res.*, *113*, D20110, doi:10.1029/2007JD009679.

Mellillo, J. M., and P. A. Steudler (1989), The effect of nitrogen fertilization on the COS and CS2 emissions from temperature forest soils, *J. Atmos. Chem.*, *9*(4), 411–417, doi:10.1016/j.agrformet.2012.11.015.

Montzka, S. A., P. Calvert, B. D. Hall, J. W. Elkins, T. J. Conway, P. P. Tans, and C. Sweeney (2007), On the global distribution, seasonality, and budget of atmospheric carbonyl sulfide (COS) and some similarities to CO_2, *J. Geophys. Res.*, *112*, D09302, doi:10.1029/2006JD007665.

Parazoo, N. C., A. S. Denning, J. A. Berry, A. Wolf, D. A. Randall, S. R. Kawa, O. Pauluis, and S. C. Doney (2011), Moist synoptic transport of CO_2 along the mid-latitude storm track, *Geophys. Res. Lett.*, *38*, L09804, doi:10.1029/2011GL047238.

Pinzon, J., M. E. Brown, and C. J. Tucker (2005), EMD Correction of orbital drift artifacts in satellite data stream, in *Hilbert-Huang Transform: Introduction and Applications*, edited by N. Huang and S. S. Shen, pp. 167–186, World Scientific Publishing Company, River Edge, N. J.

Protoschill-Krebs, G., C. Wilhelm, and J. Kesselmeier (1996), Consumption of carbonyl sulphide (COS) by higher plant carbonic anhydrase (CA), *Atmos. Environ.*, *30*(18), 3151–3156.

de Pury, D. G. G., and G. D. Farquhar (1997), Simple scaling of photosynthesis from leaves to canopies without the errors of big-leaf models, *Plant Cell Environ.*, *20*(5), 537–557.

Sandoval-Soto, L., M. Stanimirov, M. von Hobe, V. Schmitt, J. Valdes, A. Wild, and J. Kesselmeier (2005), Global uptake of carbonyl sulfide (COS) by terrestrial vegetation: Estimates corrected by deposition velocities normalized to the uptake of carbon dioxide (CO_2), *Biogeosciences*, *2*(2), 125–132.

Schwalm, C. R., et al. (2010), A model-data intercomparison of CO_2 exchange across North America: Results from the North American Carbon Program site synthesis, *J. Geophys. Res.*, *115*, G00H05, doi:10.1029/2009JG001229.

Seibt, U., L. Wingate, J. Lloyd, and J. A. Berry (2006), Diurnally variable $\delta^{18}O$ signatures of soil CO_2 fluxes indicate carbonic anhydrase activity in a forest soil, *J. Geophys. Res.*, *111*, G04005, doi:10.1029/2006JG000177.

Seibt, U., J. Kesselmeier, L. Sandoval-Soto, U. Kuhn, and J. A. Berry (2010), A kinetic analysis of leaf uptake of COS and its relation to transpiration, photosynthesis and carbon isotope fractionation, *Biogeosciences*, *7*(1), 333–341.

Sellers, P. J. (1985), Canopy reflectance, photosynthesis and transpiration, *Int. J. Remote Sens.*, *6*(8), 1335–1372.

Sellers, P. J., Y. Mintz, Y. C. Sud, and A. Dalcher (1986), A simple biosphere model (Sib) for use within general-circulation models, *J. Atmos. Sci.*, *43*(6), 505–531.

Sellers, P. J., J. A. Berry, G. J. Collatz, C. B. Field, and F. G. Hall (1992), Canopy reflectance, photosynthesis, and transpiration .3. A reanalysis using improved leaf models and a New canopy integration scheme, *Remote Sens. Environ.*, *42*(3), 187–216.

Sellers, P. J., D. A. Randall, G. J. Collatz, J. A. Berry, C. B. Field, D. A. Dazlich, C. Zhang, G. D. Collelo, and L. Bounoua (1996a), A revised land surface parameterization (SiB2) for atmospheric GCMs .1. Model formulation, *J. Climate*, *9*(4), 676–705.

Sellers, P. J., et al. (1996b), Comparison of radiative and physiological effects of doubled atmospheric CO_2 on climate, *Science*, *271*(5254), 1402–1406.

Stimler, K., S. A. Montzka, J. A. Berry, Y. Rudich, and D. Yakir (2010), Relationships between carbonyl sulfide (COS) and CO_2 during leaf gas exchange, *New Phytol.*, *186*(4), 869–878.

Stimler, K., J. A. Berry, S. A. Montzka, and D. Yakir (2011), Association between Carbonyl Sulfide Uptake and 18Δ during Gas Exchange in C3 and C4 Leaves, *Plant Physiology*, *157*(1), 509–517, doi:10.1104/pp.111.176578.

Stimler, K., J. A. Berry, and D. Yakir (2012), Effects of carbonyl sulfide and carbonic anhydrase on stomatal conductance, *Plant Physiol.*, *158*(1), 524–530.

Suntharalingam, P., A. J. Kettle, S. M. Montzka, and D. J. Jacob (2008), Global 3-D model analysis of the seasonal cycle of atmospheric carbonyl sulfide: Implications for terrestrial vegetation uptake, *Geophys. Res. Lett.*, *35*, L19801, doi:10.1029/2008GL034332.

Toon, O. B., et al. (2010), Planning, implementation, and first results of the Tropical Composition, Cloud and Climate Coupling Experiment (TC4), *J. Geophys. Res.*, *115*, D00J04, doi:10.1029/2009JD013073.

Tucker, C. J., J. E. Pinzon, M. E. Brown, D. A. Slayback, E. W. Pak, R. Mahoney, E. F. Vermote, and N. El Saleous (2005), An extended AVHRR 8-km NDVI dataset compatible with MODIS and SPOT vegetation NDVI data, *Int. J. Remote Sens.*, *26*(20), 4485–4498.

Van Diest, H., and J. Kesselmeier (2008), Soil atmosphere exchange of carbonyl sulfide (COS) regulated by diffusivity depending on water-filled pore space, *Biogeosciences*, *5*(2), 475–483.

Vay, S. A., et al. (2003), Influence of regional-scale anthropogenic emissions on CO_2 distributions over the western North Pacific, *J. Geophys. Res.*, *108*(D20), 8801, doi:10.1029/2002JD003094.

Vidale, P. L., and R. Stockli (2005), Prognostic canopy air space solutions for land surface exchanges, *Theor. Appl. Climatol.*, *80*(2–4), 245–257.

Wang, Y. P., and R. Leuning (1998), A two-leaf model for canopy conductance, photosynthesis and partitioning of available energy I: Model description and comparison with a multi-layered model, *Agr. Forest Meteorol.*, *91*(1–2), 89–111.

van der Werf, G. R., J. T. Randerson, G. J. Collatz, and L. Giglio (2003), Carbon emissions from fires in tropical and subtropical ecosystems, *Global Change Biol.*, *9*(4), 547–562.

Wingate, L., U. Seibt, K. Maseyk, J. Ogee, P. Almeida, D. Yakir, J. S. Pereira, and M. Mencuccini (2008), Evaporation and carbonic anhydrase activity recorded in oxygen isotope signatures of net CO_2 fluxes from a Mediterranean soil, *Global Change Biol.*, *14*(9), 2178–2193.

Wohlfahrt, G., F. Brilli, L. Hortnagl, X. B. Xu, H. Bingemer, A. Hansel, and F. Loreto (2012), Carbonyl sulfide (COS) as a tracer for canopy photosynthesis, transpiration and stomatal conductance: potential and limitations, *Plant Cell Environ.*, *35*(4), 657–667.

Yi, Z. G., X. M. Wang, G. Y. Sheng, D. Q. Zhang, G. Y. Zhou, and J. M. Fu (2007), Soil uptake of carbonyl sulfide in subtropical forests with different successional stages in south China, *J. Geophys. Res.*, *112*, D08302, doi:10.1029/2006JD008048.